

# Monte Carlo simulations of flexible polyanions complexing with whey proteins at their isoelectric point

R. de Vries

Laboratory of Physical Chemistry and Colloid Science, and Food Physics Group,  
Dept. Agrotechnology and Food Sciences, Wageningen University, P.O. Box 8038,  
6700 EK Wageningen, The Netherlands

(Received 1 October 2003; accepted 17 November 2003)

Electrostatic complexation of flexible polyanions with the whey proteins  $\alpha$ -lactalbumin and  $\beta$ -lactoglobulin is studied using Monte Carlo simulations. The proteins are considered at their respective isoelectric points. Discrete charges on the model polyelectrolytes and proteins interact through Debye–Hückel potentials. Protein excluded volume is taken into account through a coarse-grained model of the protein shape. Consistent with experimental results, it is found that  $\alpha$ -lactalbumin complexes much more strongly than  $\beta$ -lactoglobulin. For  $\alpha$ -lactalbumin, strong complexation is due to localized binding to a single large positive “charge patch,” whereas for  $\beta$ -lactoglobulin, weak complexation is due to diffuse binding to multiple smaller charge patches.

© 2004 American Institute of Physics. [DOI: 10.1063/1.1641003]

## INTRODUCTION

Complexes of globular proteins and flexible polyelectrolytes are used, for example, in foods, cosmetics, pharmaceuticals, and medicine.<sup>1</sup> A deeper understanding of complexation in mixtures of globular proteins and flexible polyelectrolytes is of considerable technological importance. Complexation sensitively depends on the solution  $pH$  and ionic strength. This dependence has been systematically studied by Dubin and co-workers<sup>2,3</sup> for mixtures of globular proteins and highly charged synthetic polyelectrolytes. They have identified two critical  $pH$  values that sensitively depend on the ionic strength. A schematic phase diagram for the case of complexation with a polyanion is given in Fig. 1.

Soluble complexes start forming at a first critical  $pH$  value called  $pH_c$ , that is roughly independent of the protein/polyelectrolyte ratio. This value characterizes the incipient binding of a single protein to the polyelectrolyte chain. Macroscopic phase separation occurs at a second critical  $pH$  value called  $pH_\phi$ , that does depend on the protein/polyelectrolyte ratio.

Because of the strong dependence on  $pH$  and ionic strength it is usually assumed that, at least to a large extent, complexation is caused by electrostatic protein–polyelectrolyte interactions. However, for a number of systems it has been reported that soluble complexes still form when the protein and polyelectrolyte carry the same net charge.<sup>2–9</sup> Such complexation “on the wrong side” of the protein isoelectric point has been attributed to “charge patches” on the protein surface that have a sign opposite to that of the average protein charge.<sup>2</sup> Similar arguments have been used to explain the retention of proteins on ion-exchange columns, under conditions where the column material and the protein carry the same net charge.<sup>10,11</sup>

In the present paper, we consider the complexation of globular proteins with flexible polyelectrolytes under conditions where “charge patches,” or more generally, the hetero-

geneity of the protein surface charge distribution, presumably plays an important role.

Complexation of flexible and semiflexible polyelectrolytes with homogeneous, oppositely charged spheres is addressed in many recent theoretical<sup>12–20</sup> and computer simulation<sup>21–26</sup> studies. Only a few studies deal with the effects of surface charge heterogeneity. Polyelectrolyte adsorption on flat, heterogeneously charged surfaces has been studied by Muthukumar and co-workers<sup>27</sup> using Monte Carlo simulations. They found that polyelectrolytes may adsorb on surfaces with the same sign of the net charge, if surface charge heterogeneities are strong enough. Complexation of flexible polyelectrolytes with inhomogeneously charged spheres has been studied by Carlsson *et al.*,<sup>28</sup> again using Monte Carlo simulations. The inhomogeneously charged spheres had a surface charge distribution, mimicking that of lysozyme. These authors found a highly inhomogeneous distribution of the adsorbed polyelectrolyte segments over the surface of the spheres. Complexation of polyelectrolytes and spheres of similar net charge was only observed if an additional nonelectrostatic, short-ranged attraction was introduced between the spheres and the polyelectrolytes.

Recently, we have addressed<sup>29</sup> the problem of polyelectrolyte adsorption on randomly charged surfaces, using existing theory for homopolymer adsorption on annealed random surfaces.<sup>30,31</sup> In agreement with Muthukumar, we found that polyelectrolyte adsorption on surfaces with the same net charge is possible if the heterogeneity of the surface charge distribution is strong enough. The theory was also applied to protein–polyelectrolyte complexes. Analytical estimates for  $pH_c$  were obtained by viewing the heterogeneous protein surface as a randomly charged surface. The estimates were consistent with our experimental data<sup>8</sup> for mixtures of the whey protein  $\beta$ -lactoglobulin and the weakly anionic polysaccharide gum arabic.

It is gratifying that a coarse representation of the complex protein surface as an infinite, annealed randomly

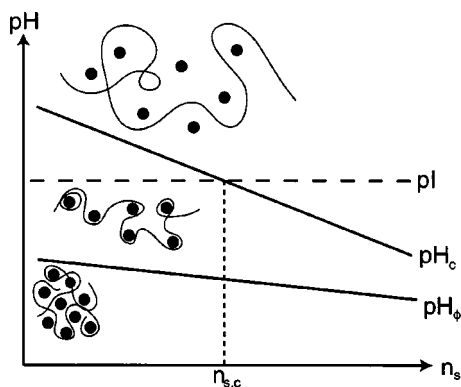


FIG. 1. Schematic phase diagram for polyanion interacting with globular protein as a function of  $pH$  and ionic strength  $n_s$ . Below a first critical value  $pH_c$ , the protein and polyanion start forming soluble complexes. At  $pH$  values below  $pH_\delta$ , macroscopic phase separation occurs. Soluble complexes form “at the wrong side” of the protein isoelectric point below a critical ionic strength  $n_{s,c}$ , that also characterizes the strength of interaction of a given protein–polyelectrolyte pair.

charged surface gives values that are of the right order of magnitude. However, the approach is extremely crude and leaves many more detailed questions unanswered. One of these questions is suggested by recent experimental results on mixtures of the whey proteins  $\alpha$ -lactalbumin and  $\beta$ -lactoglobulin with the weakly anionic polysaccharide gum arabic.<sup>8,9</sup> At low ionic strength, both proteins start complexing with gum arabic above their isoelectric point, but  $\alpha$ -lactalbumin does so to a much larger extent, and at much larger ionic strengths than  $\beta$ -lactoglobulin. The question is, if electrostatics does indeed dominate the complexation behavior, is it possible to relate differences in the complexation behavior to differences in the distribution of the “charge patches” over the surfaces of  $\alpha$ -lactalbumin and  $\beta$ -lactoglobulin?

In the vicinity of the protein isoelectric point, the interaction strength of a particular protein–polyelectrolyte pair is conveniently characterized in terms of a critical ionic strength  $n_{s,c}$  below which soluble complexes form “on the wrong side” of the protein isoelectric point. As indicated in the schematic phase diagram of Fig. 1, at this ionic strength,  $pH_c = pI$ , where  $pI$  is the protein isoelectric point. Our previous analytical estimates<sup>29</sup> suggest a linear dependency on the polyelectrolyte linear charge density  $\nu$  (elementary charges  $e$  per unit length):

$$n_{s,c} \propto \nu. \quad (1)$$

For  $\beta$ -lactoglobulin and gum arabic,  $n_{s,c} \approx 0.012$  M. Stronger binding for  $\beta$ -lactalbumin and gum arabic is reflected in a much larger value of the critical ionic strength:  $n_{s,c} \approx 0.08$  M. Complexation of serum albumin with synthetic polyelectrolytes of high linear charge density has been studied extensively by Dubin and co-workers. For these systems, critical ionic strengths are even higher.

In the present paper, using Monte Carlo simulations, we estimate critical ionic strengths for short flexible polyanions of varying, but low, linear charge density, complexing with the whey proteins  $\alpha$ -lactalbumin and  $\beta$ -lactoglobulin. The question whether it is possible to explain differences in the

complexation behavior of these proteins in terms of differences in the distribution of their “charge patches” is addressed by studying the nonuniform distribution of the polyanion center of mass around the two proteins.

## COMPUTATIONAL METHODS

In order to emphasize the generic, electrostatic nature of the complexation we do not use full atomistic modeling. Instead we use simple coarse grained models for both the polyelectrolyte and the protein. Nonbonded interactions that are taken into account are only electrostatics and excluded volume. The systems are weakly charged: the proteins are at their isoelectric points and the polyelectrolytes are assumed to have low linear charge densities (below one elementary charge  $e$  per nm). The electrostatics can then be dealt with in the linear Debye–Hückel approximation. Accounting for the effects of the low dielectric constant of the protein requires solving the full Debye–Hückel equation for our coarse grained model, which is still computationally demanding.

The main effect of the low dielectric constant of the protein is to enhance electrostatic interactions that take place close to its surface. The enhancement can be easily computed within the Debye–Hückel approximation for an infinite, flat interface between a bulk electrolyte solution and a low dielectric material. For that case, the enhancement also has a direct interpretation in terms of image charges. If the dielectric contrast is large, the surface enhancement of the interaction energy of two elementary charges next to the surface amounts to a factor of 2.<sup>32</sup> For the fuzzy, curved and finite dielectric interface between the protein and the electrolyte solution, the factor of 2 presumably is an upper bound to the true enhancement. Here we use a pragmatic approach that tries to account for the effect of the low dielectric constant of the protein at the crudest level.

## Polyelectrolyte

Although we expect that generic electrostatic effects dominate the complexation behavior, molecular details certainly do matter. The strength of binding is expected to be proportional to the number of protein–polyelectrolyte electrostatic bonds that can be simultaneously formed. It is also expected to depend sensitively on the distance of closest approach of oppositely charged groups. Aspects of the polyelectrolyte molecular geometry that are therefore expected to be important are the overall chain stiffness, as well as the local freedom of movement of the charged groups. We here consider the limiting case of a polyelectrolyte that can maximally exploit the “electrostatic complementarity” with the protein surface. The single, (short) polyanion is modeled as a chain of  $N_{\text{mon}} = 20$  spheres (monomers) of radius  $R_{\text{mon}} = 2.5$  Å, connected by harmonic springs, with a bond energy

$$U_{\text{bond}} = \frac{1}{2} \sum_{i=1}^{N_{\text{mon}}-1} k_{\text{bond}} (r_{i,i+1}/r_{\text{bond}} - 1)^2, \quad (2)$$

where  $r_{i,i+1}$  is the distance between monomer  $i$  and  $i+1$ . We do not take into account any bending energy between consecutive segments. The model polyelectrolyte is therefore intrinsically flexible. Equilibrium bond distances are  $r_{\text{bond}}$

$= 10 \text{ \AA}$ , and the bond spring constant is given a low value of  $k_{\text{bond}} = 1 k_B T$ . This implies that bond distances fluctuate, the root-mean-square bond distance being of the order of  $r_{\text{bond}}$ . Both the chain flexibility and the bond distance fluctuations allow for maximal “electrostatic complementarity” with the protein surface.

Each monomer carries a charge  $\alpha_{\text{mon}}$ , in units of elementary charges  $e$ . The linear charge density of the model polyelectrolyte is  $\nu \approx \alpha_{\text{mon}}/r_{\text{bond}}$ . This is only approximately correct because of the bond distance fluctuations. Most of the monomer–monomer interactions presumably take place sufficiently far away from the protein surface, hence we neglect the influence of the low dielectric constant of the protein on the electrostatic monomer–monomer interactions. The electrostatic interaction energy of the monomers is approximated by that of a collection of Debye–Hückel point charges. Their excluded volume interaction energy is approximated by a simple  $r^{-12}$  term. This gives a monomer–monomer interaction energy (in units of  $k_B T$ ) of

$$U_{\text{int,mon}} = l_B \sum_{j=1, i < j}^{j=N_{\text{mon}}} \alpha_{\text{mon}}^2 \frac{\exp(-\kappa r_{ij})}{r_{ij}} + \sum_{j=1, i < j}^{j=N_{\text{mon}}} \left( \frac{2R_{\text{mon}}}{r_{ij}} \right)^{12}, \quad (3)$$

where  $r_{ij}$  is the distance between the center of mass of monomers  $i$  and  $j$ . The Bjerrum length is  $l_B = e^2/\epsilon k_B T$ ,  $\epsilon$  is the solvent dielectric constant. For water, at room temperature,  $l_B \approx 0.7 \text{ nm}$ . We restrict ourselves to monovalent electrolytes, whence the Debye screening length of the electrostatic interactions is given by  $\kappa^{-1} = (8\pi l_B n_s)^{-1/2}$ , where  $n_s$  is the concentration of monovalent electrolyte.

### Protein

Proteins of  $N_{\text{res}}$  residues with  $N_{\text{ch}}$  charged groups are modeled as rigid bodies with no internal degrees of freedom, consisting of  $N_{\text{res}}$  uncharged spheres of radius  $R_{\text{res}} = 4 \text{ \AA}$ , and  $N_{\text{ch}}$  charged spheres of radius  $R_{\text{ch}} = 1.5 \text{ \AA}$  and charge  $\alpha_i$  for charged group  $i$ , in terms of elementary charges  $e$ . The value for  $R_{\text{ch}}$  is used as a parameter setting the distance of closest approach between polyelectrolyte and protein charges, rather than as an approximation of the true size of the charged groups. Each uncharged sphere represents the excluded volume of a single protein residue. Coordinates of the charged and uncharged spheres are derived from crystal structures taken from the Protein Data Bank (entry 1 hfy for  $\alpha$ -lactalbumin,<sup>33</sup> and entry 1 beb for  $\beta$ -lactoglobulin<sup>34</sup>), in the following way. For each residue, the position of the excluded volume sphere is taken to be the average of the positions of the main chain atoms of that residue (N,CA,C,O). In our simulations, for  $\beta$ -lactoglobulin, we use the crystal structure of the dimer, as is appropriate for  $pH$  values around the isoelectric point of this protein.

Positions of the charged spheres were taken to be the actual positions of the charged groups in the crystal structure. For groups where the charge is distributed between several atoms, we choose one of them. With this convention, the positively charged groups are LYS.NZ, ARG.NH1,

HIS.ND1, and the terminal nitrogen. Negatively charged groups are GLU.OE1, ASP.OD1, and the terminal oxygen, OXT.

Around the isoelectric point, the majority of the charged groups of the proteins is dissociated to a considerable extent. In view of the uncertainty in the interaction strength associated with the enhancement of the electrostatic interaction by the low dielectric constant of the protein, using detailed values for the dissociation of each of the charged groups would not make the final results more reliable. To be consistent in our approximations, we instead use the following crude prescription: all positively charged groups are given the same degree of dissociation  $\alpha_{\text{pos}} = +1$ . Then a single degree of dissociation  $\alpha_{\text{neg}}$  for all negatively charged groups is chosen, such that the net charge of the model protein is zero. For both proteins, there are more negatively than positively charged groups, hence  $|\alpha_{\text{neg}}| < 1$ .

### Protein–polyelectrolyte interaction

The electrostatic interaction energy of the polyelectrolyte monomers with charges on the protein surface is again approximated by the interaction energy of a set of Debye–Hückel point charges. The enhancement of the electrostatic interactions close to the protein surface due to the low dielectric constant of the protein is taken into account at the crudest level by using an enhancement of a factor of 2, the value for interactions at an infinitely large flat interface. Monomer-charge and monomer-residue excluded volume is again taken into account through  $r^{-12}$  potentials. This gives the final expression for the polyelectrolyte–protein interaction energy,

$$U_{\text{int,prot}} = 2l_B \sum_{i=1}^{N_{\text{mon}}} \sum_{j=1}^{N_{\text{ch}}} \alpha_{\text{mon}} \alpha_j \frac{\exp(-\kappa r_{ij})}{r_{ij}} + \sum_{i=1}^{N_{\text{mon}}} \sum_{j=1}^{N_{\text{ch}}} \left( \frac{R_{\text{ch}} + R_{\text{mon}}}{r_{ij}} \right)^{12} + \sum_{i=1}^{N_{\text{mon}}} \sum_{j=1}^{N_{\text{res}}} \left( \frac{R_{\text{res}} + R_{\text{mon}}}{r_{ij}} \right)^{12}. \quad (4)$$

In the first two terms  $r_{ij}$  is the distance between the center of mass of monomer  $i$  and charge  $j$  on the protein surface, in the last term  $r_{ij}$  is the distance between monomer  $i$  and the sphere representing protein residue  $j$ .

The maximum strength of an electrostatic bond (between fully dissociated, oppositely charged groups) in our system is  $2l_B/(R_{\text{ch}} + R_{\text{mon}}) \approx 0.35 k_B T$ . Our model system therefore corresponds to a situation where the formation of soluble complexes involves multiple (relatively weak) electrostatic bonds. For real protein–polyelectrolyte systems, the maximum bond strength may be significantly higher or lower, depending on the nature of the groups involved.

### Simulation method

Our model system consists of a single model protein (for  $\alpha$ -lactalbumin) or a single model protein dimer (for  $\beta$ -lactoglobulin) and a single model polyelectrolyte chain. The proteins are fixed in the center of a cubic simulation box



with sides of  $L_{\text{box}} = 40$  nm. Sequences of polyelectrolyte configurations are generated using the Metropolis Monte Carlo algorithm in the canonical ensemble. Periodic boundary conditions are employed, interactions are truncated using the minimum image convention.

Three kinds of moves are used to displace polyelectrolyte monomers. In an elementary displacement move, a single, randomly selected monomer is moved to a new position. The new position is uniformly sampled in a cubic box with sides  $\Delta l_{\text{dis}}$ , centered on the old position of the monomer. In a reptation move, we randomly select either the first or the last monomer of the chain. The new configuration is obtained by removing this monomer and adding a new monomer at the other end of the chain. The position of the new monomer is uniformly sampled in a cubic box with sides  $\Delta l_{\text{rept}}$ , centered on the monomer at the other end of the chain. Finally, in a translation move, the entire polyelectrolyte chain is translated. The new center of mass of the polyelectrolyte is uniformly sampled in cubic box with sides  $\Delta l_{\text{trans}}$  centered on the old center of mass of the polyelectrolyte.

Elementary displacement moves and reptation moves are chosen with the same probability, translation moves were attempted with a low probability of  $P = 0.01$ . The parameters for the trial moves are  $\Delta l_{\text{dis}} = 0.5$  nm,  $\Delta l_{\text{rept}} = 2.0$  nm, and  $\Delta l_{\text{trans}} = 20$  nm. Each simulation consists of  $5 \times 10^6$  attempted trial moves per monomer, on an equilibrated initial configuration. Configurations were saved every  $10^3$  attempted trial moves per particle. Statistical uncertainties were estimated using the method of block averages.<sup>35</sup>

In order to estimate critical salt concentrations, from the saved configurations, we compute the average electrostatic interaction energy  $\langle E_{\text{el}} \rangle$  of the polyelectrolyte with the protein for each run,

$$\langle E_{\text{el}} \rangle = 2l_B \sum_{i=1}^{N_{\text{mon}}} \sum_{j=1}^{N_{\text{ch}}} \alpha_{\text{mon}} \alpha_j \frac{\exp(-\kappa r_{ij})}{r_{ij}}. \quad (5)$$

For selected runs, we also compute the polyelectrolyte center of masses of all saved configurations. These are used to make plots that give an impression of the distribution of the polyelectrolyte center of mass.

## RESULTS AND DISCUSSION

The average electrostatic interaction energy of the  $\beta$ -lactoglobulin dimer and short polyanions is shown in Fig. 2, as a function of the salt concentration, and for a range of polyelectrolyte linear charge densities. For the most highly charged polyanions, a decrease in the electrostatic interaction energy, indicates the onset of complexation at ionic strengths on the order of  $10^{-2}$  M. For the more weakly charged polyanions, the onset of complexation becomes progressively less pronounced and shifts to lower ionic strengths.

For all cases the onset of complexation upon decreasing the ionic strength is continuous, rather than discontinuous. Adsorption of infinitely long polyelectrolytes on infinitely large charged surfaces may be considered as a kind of phase transition, with a true discontinuity in the behavior as a function of ionic strength. However, protein–polyelectrolyte

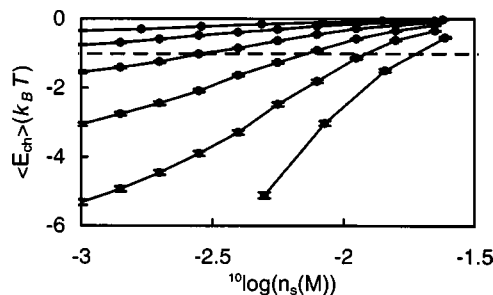


FIG. 2. Electrostatic interaction energy  $\langle E_{\text{el}} \rangle$  of  $\beta$ -lactoglobulin dimer with short model polyanions of various linear charge densities, as a function of the ionic strength  $n_s$ . The dashed line indicates the threshold of  $-1 k_B T$  that is used as the criterion for the onset of the formation of soluble complexes. Polyelectrolyte linear charge densities, from right to left,  $\alpha_{\text{mon}} = -1.0, -0.9, -0.8, -0.7, -0.6, -0.5$ .

complexes are stabilized by at most  $O(10)$  electrostatic bonds, hence there is no sharp transition. It should be noted however, that we consider polyanions of low linear charge density. For highly charged polyelectrolytes the transition may still be much sharper than what we find here.

The gradual onset of complexation makes it difficult to define a critical ionic strength at which complexation starts, in our system. Since the simulations are rather approximate anyway, we do not pursue the issue of a precise definition of  $pH_c$  any further here. As an approximation to experimentally determined critical ionic strengths, we here simply use the value at which the average attractive protein–polyelectrolyte interaction energy equals the thermal energy,  $k_B T$ . A similar criterion is applied by Grymonpré *et al.*<sup>36</sup> for estimating  $pH_c$  values from numerical solutions of the Poisson–Boltzmann equation around serum albumin. In Fig. 2, the boundary of  $-1 k_B T$  is indicated by the dashed line. Note that the most weakly charged polyanions do not exhibit electrostatic attraction larger than  $k_B T$  for any ionic strength.

Approximate critical ionic strengths for  $\beta$ -lactalbumin and  $\alpha$ -lactoglobulin as a function of the linear charge density of the (short) polyanions are shown in Fig. 3. Consistent with the experimental results for complexation with gum arabic,<sup>8,9</sup> critical ionic strengths are much larger for  $\beta$ -lactalbumin than for  $\alpha$ -lactoglobulin. Furthermore, in agreement with our previous analytical estimate for polyelectrolytes adsorbing on infinite randomly charged surfaces,<sup>29</sup> the dependence of the critical ionic strength on the polyelectrolyte linear charge density is linear. However, the protein surfaces are finite, and

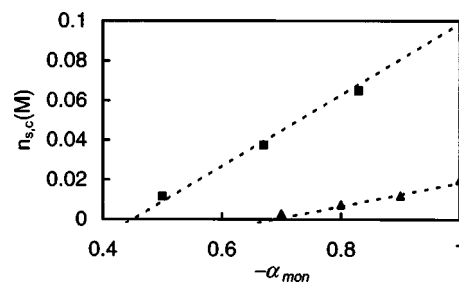


FIG. 3. Estimated critical ionic strengths for  $\alpha$ -lactalbumin and for  $\beta$ -lactoglobulin dimers complexing with short polyanions, as a function of the polyanion linear charge density  $\alpha_{\text{mon}}$ .

as a consequence, below a certain critical polyanion linear charge density, the attractions never exceed  $k_B T$ . In terms of our approximate criterion for the onset of complexation, this means that there is a critical linear charge density below which there is no complexation at all:

$$n_{s,c} \approx n_{s,0} (|\alpha_{\text{mon}}| / \alpha_{\text{crit}} - 1) \quad \text{for } |\alpha_{\text{mon}}| > \alpha_{\text{crit}}. \quad (6)$$

For  $\alpha$ -lactalbumin,  $n_{s,0} \approx 0.08$  M and  $\alpha_{\text{crit}} \approx 0.45$ , for  $\beta$ -lactoglobulin,  $n_{s,0} \approx 0.04$  M and  $\alpha_{\text{crit}} \approx 0.7$ . A direct comparison with the experimental data for complexation with gum arabic is difficult, for a number of reasons. Gum arabic is a complicated, branched, polysaccharide which also contains a proteinaceous part. For such a complicated system it is not clear to what extent nonelectrostatic forces contribute to the observed complexation behavior. Furthermore, branched chains may give critical salt concentrations that differ from those of the linear chains that we study here. Also, we consider the limit of very flexible chains. For gum arabic, chain stiffness might also affect critical salt concentrations. Nevertheless, typical differences between the experimental critical salt concentrations for the two proteins ( $n_{s,c} \approx 0.08$  M for  $\alpha$ -lactalbumin as compared to  $n_{s,c} \approx 0.012$  M for  $\beta$ -lactoglobulin) are of the same order of magnitude as the differences between the critical salt concentrations estimated from the simulations, for reasonable linear charge densities on the order of one elementary charge  $e$  per nm.

Note that even for model linear polyelectrolytes of low linear charge density the simulations are only semiquantitative. This is because critical ionic strengths depend sensitively on the magnitude of the electrostatic interactions, and since we have made rather drastic approximations in modeling the latter. Also, practically all real polyelectrolytes presumably have some intrinsic stiffness, and often steric constraints will to some degree prevent polyelectrolyte charged groups from coming close to oppositely charged protein groups. Finally, the crude approximation that we use to include the effect of the low protein dielectric constant, overestimates the importance of electrostatic attractions. In short, our simulations presumably give an approximate upperbound to the strength of electrostatic binding for real systems.

Carlsson *et al.*<sup>28</sup> use a model very similar to ours, but yet their simulation results show that for lysozyme, purely electrostatic complexation only occurs with flexible polyelectrolytes of opposite net charge. This may be related to our finding that, around the isoelectric point, there are large differences in the strength of electrostatic polyelectrolyte binding of different proteins. Possibly lysozyme binds even weaker around its isoelectric point than  $\beta$ -lactoglobulin. Furthermore, Carlsson *et al.* do not allow for large fluctuations of bond distances, they include a bending energy between consecutive segments, and do not include any enhancement of the electrostatic interactions near the protein surface. All of these factors weaken the electrostatic binding affinity as compared to our simulation results.

Finally consider the question, why  $\alpha$ -lactalbumin binds so much stronger than  $\beta$ -lactoglobulin. Elsewhere,<sup>37</sup> we have performed a statistical analysis of the distribution of "charge patches" over the surfaces of, respectively,  $\alpha$ -lactalbumin

and  $\beta$ -lactoglobulin. It was found that for  $\alpha$ -lactalbumin, significantly more of its positively charged groups were part of large charge patches than for  $\beta$ -lactoglobulin. Furthermore,  $\alpha$ -lactalbumin was found to have one particularly large charge patch, consisting of a cluster of six positively charged groups.<sup>38</sup> Therefore it was suggested that strong binding for  $\alpha$ -lactalbumin was possibly due to this single large charge patch, whereas weak binding for  $\beta$ -lactoglobulin was possibly due to binding to multiple small patches.

This hypothesis can now be tested against the simulation results. Localization of binding is visualized via the distribution of the center of mass of the flexible polyelectrolyte. A visual impression of the center-of-mass distribution is obtained by representing the center of mass of each saved polyelectrolyte configuration by a dot. We compare the behavior of the two proteins at a fixed polyelectrolyte linear charge density of  $\alpha_{\text{mon}} = -1.0$  and an ionic strength of  $n_s = 0.01$  M. Figure 4(a) shows a representative configuration of a polyanion bound to the  $\beta$ -lactoglobulin dimer. The distribution of the polyelectrolyte center of mass is visualized in Fig. 4(b). Most of the polyelectrolytes bind on one side of the dimer. On this side the distribution is rather diffuse, with a weak maximum in the middle, closest to the protein-protein interface. Not surprisingly, the side that binds the polyelectrolytes contains an excess of positively charged groups, which is compensated for, by an excess of negatively charged groups on the other side of the protein.

Other authors have also emphasized the importance of the dipolar character of globular proteins for their polyelectrolyte-binding properties, especially in connection to the often observed maximum in binding strength at low ionic strength.<sup>39</sup> This is thought to be caused by differential screening of attractive and repulsive electrostatic interactions. For bound polyelectrolyte configurations, on average, similarly charged protein and polyelectrolyte groups will be further apart than oppositely charged ones. At low ionic strength, adding salt has the effect of first screening the repulsive interactions, and then the attractive ones. Therefore, binding first increases and then decreases with increasing ionic strength.

This effect is not observed for our parameter values, although for the lowest charge densities, the curves in Fig. 2 do show a slight inflection. In order to observe a maximum in the binding strength due to differential screening we presumably would have to go to larger polyelectrolyte linear charge densities, beyond the validity of the Debye-Hückel approximation.

Next consider the polyelectrolyte center-of-mass distribution for  $\alpha$ -lactalbumin, visualized in Fig. 5(a). Not only is the binding much stronger, but, as compared to  $\beta$ -lactoglobulin, binding also occurs to a much smaller region. This region is exactly centered on the large positive charge patch that we previously identified through a statistical analysis of the  $\alpha$ -lactalbumin surface charge distribution.<sup>37</sup> This is illustrated in Fig. 5(b), which shows the crystal structure of  $\alpha$ -lactalbumin, with colored charged groups. A comparison of this figure with Fig. 5(a) also illustrates the level of coarse graining involved in our model. Five out of the six charged groups that make up the largest

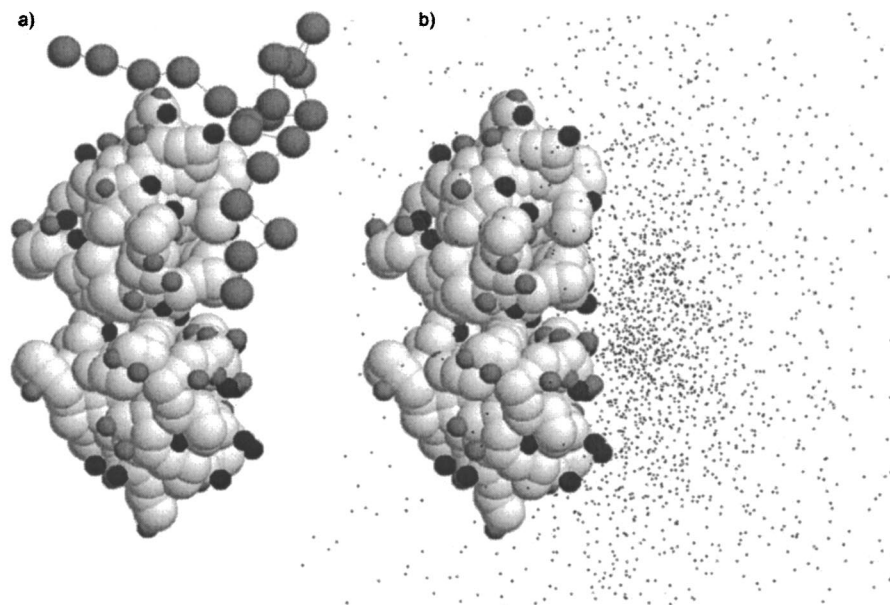


FIG. 4. Complexation of short polyanion of linear charge density  $\alpha_{\text{mon}} = -1.0$  at an ionic strength of  $n_s = 0.01$  M with  $\beta$ -lactoglobulin dimer. Protein excluded volume spheres are white, negatively charged protein groups are gray, and positively charged protein groups are black. (a) Typical configuration of adsorbed polyanion. (b) Visualization of the polyanion center-of-mass distribution. Each spot represents the polyanion center of mass of a saved configuration.

patch for  $\alpha$ -lactalbumin have been indicated by arrows, a further one is at the back side of the protein.

Clearly, this single largest charge patch is responsible for most of the binding for  $\alpha$ -lactalbumin. On the other hand, for  $\beta$ -lactoglobulin, binding occurs to multiple smaller charge patches. The binding region includes many negative charges too, that lower its “effective” positive surface charge density.

On the basis of our results on the mode of binding for these two proteins, it may be possible to develop simple electrostatic models that can be used in analyzing the complexation in more detail. For example, for both  $\alpha$ -lactalbumin and  $\beta$ -lactoglobulin, effective dipole models

could be developed that are somewhat more detailed than the schematic dipole model of Hattori *et al.*<sup>39</sup> An attractive possibility to study the phenomenon of the nonmonotonic salt dependence of the binding strength in more detail is to use numerical self-consistent-field theory. Then one can account for both strong electrostatic interactions at the Poisson–Boltzmann level, and for the important configurational entropy and self-interaction of the polyelectrolyte.

Here we have restricted ourselves to monovalent electrolyte. An interesting issue that has not yet been studied extensively in model experiments is the influence of multivalent ions on protein–polyelectrolyte binding. Most likely, for proteins around the isoelectric point, adding multivalent cations

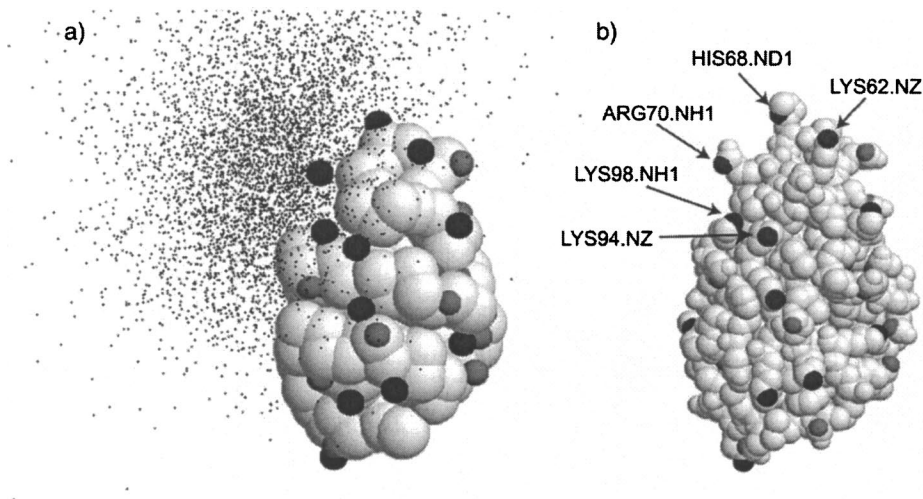


FIG. 5. Complexation of short polyanion of linear charge density  $\alpha_{\text{mon}} = -1.0$  at an ionic strength of  $n_s = 0.01$  M with  $\alpha$ -lactalbumin. Negatively charged protein groups are gray, positively charged protein groups are black. (a) Visualization of the polyanion center-of-mass distribution. Each spot represents the polyanion center of mass of a saved configuration. Protein excluded volume spheres are white. (b) Crystal structure of  $\alpha$ -lactalbumin (pdb entry, 1hfy) used in the construction of the coarse grained protein model. Uncharged atoms are white. Arrows point to five out of the six positively charged atoms that make up the largest “positive patch” on the surface of the protein. A last one is on the back side of the protein.



would favor the binding of polyanions and oppose the binding of polycations. The asymmetry of binding for polyanions and polycations to proteins at their isoelectric point also exists in the absence of multivalent ions, in view of the different spatial distribution of the positive and negative charges over the protein surface. Adding multivalent ions would enhance this asymmetry, an effect that could be included in our approximate model by explicitly including these multivalent ions, still using the Debye–Hückel approximation to account for screening by the monovalent electrolyte.

Finally, our results show that a simple statistical analysis of the surface charge density is already sufficient for identifying potential polyelectrolyte binding regions. This may be complemented by numerical solutions of the Poisson–Boltzmann equation around molecular protein models.<sup>36,39</sup> It should be emphasized however, that any protein-only approach can only identify possible regions of polyelectrolyte binding, and does not account for any of the polyelectrolyte properties that influence binding.

## ACKNOWLEDGMENTS

The author thanks Fanny Weinbreck and Cees de Kruiif for useful discussions.

- <sup>1</sup>C. Schmitt, C. Sanchez, S. Desobry-Banon, and J. Hardy, *Crit. Rev. Food Sci. Nutr.* **38**, 689 (1998).
- <sup>2</sup>J. M. Park, B. B. Muhoherac, P. L. Dubin, and J. Xia, *Macromolecules* **25**, 290 (1992).
- <sup>3</sup>K. W. Mattison, I. J. Brittain, and P. L. Dubin, *Biotechnol. Prog.* **11**, 682 (1995).
- <sup>4</sup>J. Xia, P. L. Dubin, Y. Kim, B. B. Muhoherac, and V. J. Klimkowski, *J. Phys. Chem.* **97**, 4528 (1993).
- <sup>5</sup>Y. Li, K. W. Mattison, P. L. Dubin, H. A. Havel, and S. L. Edwards, *Biopolymers* **38**, 527 (1996).
- <sup>6</sup>J. Y. Gao, P. L. Dubin, and B. B. Muhoherac, *Anal. Chem.* **69**, 2945 (1997).
- <sup>7</sup>K. W. Mattison, P. L. Dubin, and I. J. Brittain, *J. Phys. Chem.* **102**, 3830 (1998).
- <sup>8</sup>F. Weinbreck, R. de Vries, P. Schrooyen, and C. G. de Kruiif, *Biomacromolecules* **4**, 293 (2003).
- <sup>9</sup>F. Weinbreck and C. G. de Kruiif, in *Food Colloids, Biopolymers and Materials*, edited by E. Dickinson and T. van Vliet (Royal Society of Chemistry, Cambridge, 2003), pp. 329–336.
- <sup>10</sup>V. Lesins and E. Ruckenstein, *Colloid Polym. Sci.* **266**, 1187 (1988).
- <sup>11</sup>D. Asthagiri and A. Lenhoff, *Langmuir* **13**, 6761 (1997).
- <sup>12</sup>N. L. Marky and G. S. Manning, *Biopolymers* **31**, 1543 (1991); N. L. Marky and G. S. Manning, *J. Mol. Biol.* **254**, 50 (1995).
- <sup>13</sup>F. von Goeler and M. Muthukumar, *J. Chem. Phys.* **100**, 7796 (1994).
- <sup>14</sup>R. R. Netz and J.-F. Joanny, *Macromolecules* **32**, 9026 (1999); K. K. Kunze and R. R. Netz, *Phys. Rev. E* **66**, 011918 (2002).
- <sup>15</sup>T. T. Nguyen and B. B. Shklovskii, *J. Chem. Phys.* **114**, 5905 (2001); *Physica A* **293**, 324 (2001).
- <sup>16</sup>P. Haronska, T. A. Vilgis, R. Grottenmuller, and M. Schmidt, *Macromol. Theory Simul.* **7**, 241 (1998).
- <sup>17</sup>E. Gurovitch and P. Sens, *Phys. Rev. Lett.* **82**, 339 (1999); R. Golestanian, *ibid.* **83**, 2473 (1999).
- <sup>18</sup>S. Y. Park, R. F. Bruinsma, and W. M. Gelbart, *Europhys. Lett.* **46**, 454 (1999).
- <sup>19</sup>H. Schiessel, R. F. Bruinsma, and W. M. Gelbart, *J. Chem. Phys.* **115**, 7245 (2001).
- <sup>20</sup>L. Harnau and J.-P. Hansen, *J. Chem. Phys.* **116**, 9051 (2002).
- <sup>21</sup>C. Y. Kong and M. Muthukumar, *J. Chem. Phys.* **109**, 1522 (1998).
- <sup>22</sup>T. Wallin and P. Linse, *Langmuir* **12**, 305 (1996); *J. Phys. Chem. B* **100**, 17873 (1996); **101**, 5506 (1997).
- <sup>23</sup>T. Wallin and P. Linse, *J. Chem. Phys.* **109**, 5089 (1998).
- <sup>24</sup>M. Jonsson and P. Linse, *J. Chem. Phys.* **115**, 3406 (2001); **115**, 10975 (2001).
- <sup>25</sup>A. Akinchina and P. Linse, *Macromolecules* **35**, 5183 (2002).
- <sup>26</sup>P. Chodanowski and S. Stoll, *J. Chem. Phys.* **115**, 4951 (2001); *Macromolecules* **34**, 2320 (2001).
- <sup>27</sup>M. Ellis, C. Y. Kong, and M. Muthukumar, *J. Chem. Phys.* **112**, 8723 (2000); J. McNamara, C. Y. Kong, and M. Muthukumar, *ibid.* **117**, 5354 (2002).
- <sup>28</sup>F. Carlsson, P. Linse, and M. Malmsten, *J. Phys. Chem. B* **105**, 9040 (2001).
- <sup>29</sup>R. de Vries, F. Weinbreck, and C. G. de Kruiif, *J. Chem. Phys.* **118**, 4649 (2003).
- <sup>30</sup>T. Odijk, *Macromolecules* **23**, 1875 (2003).
- <sup>31</sup>D. Andelman and J.-F. Joanny, *Macromolecules* **24**, 6040 (1991).
- <sup>32</sup>R. R. Netz, *Phys. Rev. E* **60**, 3174 (1999).
- <sup>33</sup>A. C. Pike, K. Brew, and K. R. Acharya, *Structure (London)* **4**, 691 (1996).
- <sup>34</sup>S. Bronlow, J. H. Morais-Cabral, R. Cooper, D. R. Flower, S. J. Yewdall, I. Polikarpov, A. C. North, and L. Sawyer, *Structure (London)* **5**, 481 (1997).
- <sup>35</sup>D. Frenkel and B. Smit, *Understanding Molecular Simulation* (Academic, San Diego, CA, 1996).
- <sup>36</sup>K. R. Grynmonpre, B. A. Staggemeier, P. L. Dubin, and K. W. Mattison, *Biomacromolecules* **2**, 422 (2001).
- <sup>37</sup>R. de Vries, in *Food Colloids, Biopolymers and Materials*, edited by E. Dickinson and T. van Vliet (Royal Society of Chemistry, Cambridge, 2003), pp. 329–336.
- <sup>38</sup>This largest positive “charge patch” for  $\alpha$ -lactalbumin, as identified using the statistical analysis of Ref. 37, is centered on ARG70.NH1 and furthermore includes LYS98.NZ, HIS68.ND1, LYS94.NZ, LYS62.NZ, and LYS58.NZ of the crystal structure<sup>35</sup> with pdb entry 1HFY.
- <sup>39</sup>T. Hattori, R. Hallberg, and P. L. Dubin, *Langmuir* **16**, 9738 (2000); E. Seyrek, P. L. Dubin, C. Tribet, and E. A. Gamble, *Biomacromolecules* **4**, 273 (2003).